2007 IEEE International Conference on
Robotics and Automation
Roma, Italy, 10-14 April 2007

Real-Time Knotting and Unkotting

Hans Fuhan Shi and Shahram Payandeh

Abstract— **Suturing simulations, of which real-time knotting and unknotting are the most challenge parts, are essential to today's surgical training systems. In this paper, we present a physics-based approach to real-time simulation of deformable linear objects (DLOs) with visual and force feedback. In our suture model, which can represent the mechanical properties of a real thread such as stretching, compressing, bending, and twisting, we simulate not only external forces, but also internal forces including the friction force during knotting and unknotting. We also present how forces propagate along the suture when the user pulls it with one or two hands. We developed a simulator to allow users to grasp and smoothly manipulate a virtual thread, and to tie an arbitrary knot.**

I. Introduction

COMPUTER-BASED surgical simulations, using computers and electromechanical user interface devices, open new possibilities in surgical training, offering many benefits compared to traditional training methods. Real-time knotting and unknotting simulations, which are the key components of suturing in surgical training systems raise unique and difficult issues because of the suture's deformability, difficulty of collision detection and management, and the demanding requirements of force feedback output. In this paper, we developed a simulator in our surgical training environment to allow users to tie and untie any kind of knot.

Section II of this paper covers previous works. Section III describes the model we are using and illustrates how to calculate internal and external forces. Section IV covers how forces propagate along the suture during knotting and unknotting. Section V describes case studies and results, and section VI gives the conclusion and discusses about the future work.

II. Previous Work

There are a number of works which have made some contributions to the development of deformable linear objects (DLOs) simulation. Most of these previous models can be categorized as geometry-based models or physics-based models. In surgical training systems, because the purpose is to enable users to feel the force feedback, especially for knotting and unknotting in suturing, to make it more realistic, we need to consider both external and internal forces to determine the force output. Thus geometric models are obviously inappropriate.

H. Shi is with Experimental Robotics Laboratory, School of Engineering Science, Simon Fraser University, Burnaby, BC V5A 1S6, CANADA fuhans@ensc.sfu.ca

S. Payandeh is with Experimental Robotics Laboratory, School of Engineering Science, Simon Fraser University, Burnaby, BC V5A 1S6, CANADA shahram@ensc.sfu.ca

Some researchers have been focusing on knotting manipulation by robots. In [1], Wakamatsu, Arai and Hirai established a model of DLOs based on an extension of differential geometry, and proposed a planning method for knotting/unknotting of DLOs based on the knot theory. If the initial and the objective states of the linear object are given, all possible knotting/unknotting plans can be derived and be executed by their system. However, their proposed models can not simulate the DLOs dynamically in 3D space. In addition, their system does not allow any user interaction, and can not simulate the knotting/unknotting procedure in real-time. [2] describes a 2D DLOs dynamic model based on the differential geometry coordinates. In [3], a knot planning from observation(KPO) system is described. First, this system observes the procedure of tying a knot by a human as a sequence of movement primitives. Then, by repeating the sequence, it can tie a similar knot. The topological information of a knot is represented in a P-data representation. In [4], a topological motion planner for manipulating DLOs and tying knots using cooperating robot arms was introduced based on Probabilistic RoadMaps (PRMs).

In [5] [6] [7], a Cosserat approach of modeling DLOs based on the Cosserat theory of elastic rods has been introduced. Cosserat model is well suited for real-time applications because it needs less computation compared to finite elements models and provides a clear delineation between basic physical principles, material properties and mathematical approximations. However, in return, it yields a set of ordinary differential equations to be solved. If two end points or multiple points along the length of a suture are specified (as in the procedure of knotting or unknotting with two hands), it is significantly more difficult to solve these equations. In addition, the "shooting" technique which is mentioned in [5] makes it very difficult to integrate external forces [8].

A particle-based model of a rope is represented in [9] by overlapping spheres representing mass-points, which are connected by simple springs. Each mass-point can collide with other mass points as in the instantaneous elastic collision model, but the author only considers the linear spring forces and does not allow any user interaction. In [10], inner bending force and the gravity are taken into consideration. In [11], the author mentioned gravity, stretch/compression force, forces from bending and twisting, dissipative friction, and contact forces with environment or to self-collsion, but there is no detail about how to compute those forces.

A mass-spring model for suturing in surgical training system has been built in [12]. Torsional spring, torsional

damper, and viscous damper are mentioned in this paper, but, the author did not use them in the simulation due to the complex computation. Further more, there is no discussion about collision detection and force propagation for haptic interaction between the user and the suture model.

Our suture model is built based on all the forces mentioned in [12], and we provide a user-interface to allow users tie an arbitrary knot. Also we analyze how the forces propagate along the suture during knotting and unknotting. With the virtual coupling technique[13], we can provide very smooth force feedback to the user.

III. Model Description

For 1D element, we model our suture as a mass-spring system which consists of a sequence of mass points laying on the centreline of the suture. (see (a) of Fig. 1).

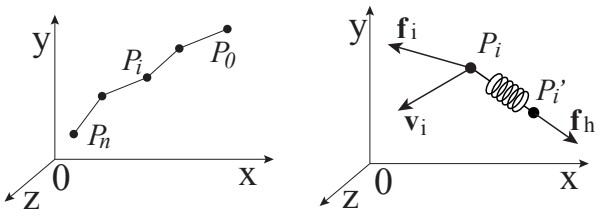

(a) *Suture Model* (b) *Virtual Coupling*

Fig. 1. Suture Model and Virtual Coupling of Haptic Device

During graphic rendering, we use cylinders as suture segments connecting two successive points. We use Euler method to calculate the shape of our suture. We first compute the total force acting at each point, P_i, and then update its position based on the computed force. Once the total force at each of the nodes has been calculated, with the interval time dt, we can obtain the velocity and position of each point.

The following part of this section explains the forces we simulate in our simulator. We can use various combinations of these forces to build different models. The springs and dampers both contribute some force to the net force $\mathbf{f}$ at each point. Different springs and dampers all behave differently and we calculate their force contributions using their own particular equations.

A. External Forces

The external forces include the gravitational force, the user input forces through haptic devices, the friction forces during knotting or unknotting, as well as the contact force with obstacles:

1) Gravity: $\mathbf{f}_g = Gm$. where $G = 9.8N/kg$, and m is the mass of the mass point.

2) User Input Force: Allowing the user to provide both input and output to the simulation in the form of forces, positions, and velocity etc, a haptic device becomes a natural interface for a dynamic simulation, which needs to calculate all the forces applied to the objects. However, a position controlled impedance style haptic device, such as PHANTOM Omni and PHANTOM Desktop from Sensable Tchenology, forces are not directly available as input variables into the model. Furthermore, the mechanical characterization and digital nature of the haptic device make the operation of directly incorporating the device as part of the simulation more challenging. To overcome these difficulties, we use virtual coupling technique which introduces a indirect layer of interaction between the mechanical device and the simulation by employing a spring-damper between a simulated body and the device end-effector (see (b) of Fig. 1). Another advantage of this technique is that we can use different constants for computing the output force for the device versus the input force for the simulated body, which makes the forces appropriate for both the haptic device and the dynamic simulation.

3) Friction Force: In this paper, we only consider coulomb and viscous friction forces during the procedure of knotting and unknotting, and we do not consider the rolling friction. We will study the static friction and focus on how to tie a knot tightly and unknot a tight knot in the future. During the simulation, we use Coulomb's model and consider each suture segment as rigid body, hence we can not bend to any angle for any instant time. From Coulomb's observations we know that: kinetic frictional force is approximately independent of contact area and velocity magnitude of the object; Coefficient of friction depends on pairs of materials. During knotting or unknotting procedure, suppose there are only two segments colliding with each other (see Fig. 2). Let μ be the

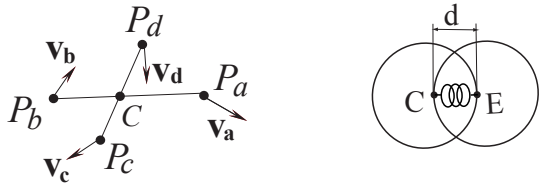

(a) *Two Sliding Segments* (b)*Two Segments Intersection*

Fig. 2. Friction during knotting / unknotting

friction constant, $\hat{\mathbf{e}}$ be the friction direction vector, $\mathbf{n}$ be the force of repulsion, then the friction $\mathbf{f}_f$ can be described as:

$$\mathbf{f}_f = \mu||\mathbf{n}||\hat{\mathbf{e}}. \tag{1}$$

To calculate the repulsion force $\mathbf{n}$, we introduce a spring-damper between the contact point C and the end point E.

$$\mathbf{n} \quad = \quad (k_{rs}(2r-d) - k_{rd}(\mathbf{v}_r \cdot \hat{\mathbf{n}}))\hat{\mathbf{n}}. \tag{2}$$

where k_{rs} is a spring constant for the repulsion force, r is the radius of the suture model, d is the distance between point C to point E (see (b) of Fig. 2), k_{rd} is the damper constant for the repulsion force, $\mathbf{v}_r$ is the relative velocity of point C with respect to point E, $\hat{\mathbf{n}}$ is the unit vector from point E to point C. We use linear interpolation to compute the velocity of a point on the segment. For example (see Fig. 2), $\mathbf{v}_c = (1-a)\mathbf{v}_a + a\mathbf{v}_b$, where a is the fraction of point C along $\overrightarrow{P_aP_b}$, $\mathbf{v}_e = (1-b)\mathbf{v}_c + b\mathbf{v}_d$, where b is the fraction of

point E along $\overrightarrow{P_cP_d}$. Then the relative velocity $\mathbf{v}_r = \mathbf{v}_c - \mathbf{v}_e$, and the friction direction vector $\hat{\mathbf{e}}$ is computed as follows:

$$\hat{\mathbf{e}} = \frac{(\mathbf{v}_r \cdot \hat{\mathbf{n}})\hat{\mathbf{n}} - \mathbf{v}_r}{||(\mathbf{v}_r \cdot \hat{\mathbf{n}})\hat{\mathbf{n}} - \mathbf{v}_r||}. \quad (3)$$

B. Internal Forces

1) Linear spring force: The linear spring force is computed by comparing the current segment length, l_i, between point, P_i and P_{i+1}, with the rest length of the segment l_r, and by projecting the resulting difference on the direction from point P_i to P_{i+1}. Then, $l_i = ||P_{i+1} - P_i||$, $\Delta l = \frac{l_i - l_r}{l_r}$, and l_r, is the rest length between point, P_i and P_{i+1}. Let $\hat{\mathbf{e}}_i$ be the unit vector from point, P_i to P_{i+1}, then,

$$\hat{\mathbf{e}}_i = \frac{P_{i+1} - P_i}{||P_{i+1} - P_i||}, \quad (4)$$

$$\mathbf{f}_s = k_l \Delta l \hat{\mathbf{e}}_i. \quad (5)$$

where k_l is the linear spring constant.

2) Linear damper: We simulate all the factors that try to stop the spring as it moves as one constant called the damping factor, k_d. This force opposes the direction of movement and is proportional to the velocity of the moving mass. When the system is at rest ($\mathbf{v} = 0$), no linear damping force is involved.

$$\mathbf{f}_d = k_d(v_{i+1} - v_i)\hat{\mathbf{e}}_i. \quad (6)$$

where $v_{i+1} = \mathbf{v}_{i+1} \cdot \hat{\mathbf{e}}_i$, $v_i = \mathbf{v}_i \cdot \hat{\mathbf{e}}_i$, k_d is the linear damper constant. v_{i+1} and v_i are the norms of the components of the velocity of point P_{i+1} and P_i on the direction $\hat{\mathbf{e}}_i$.

3) Torsional spring: The torsional spring is derived from the angle, α, between two connected segments of the rope. The basic idea is to model each two connected segments as a triangle with a spring as the hypothesis pushing the end points to the full expanded position. The length of the two connected segments remain unchanged. Only the force component orthogonal to the segments is used for the end points (See (a) of Fig. 3). Let $\hat{\mathbf{e}}_{i-1}$ and $\hat{\mathbf{e}}_i$ be the unit

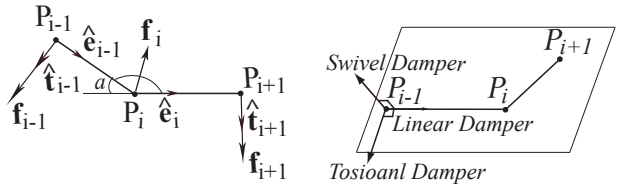

(a) *Torsional Spring* (b) *Swivel Damper*

Fig. 3. Torsional Spring and Swivel Damper

vectors with directions from point, P_{i-1} to P_i, and from P_i to P_{i+1}, respectively. Let $\hat{\mathbf{t}}_{i-1}$ and $\hat{\mathbf{t}}_{i+1}$ be the unit vectors with directions the same as the torsional force applied at the two endpoints and therefore, orthogonal to $\hat{\mathbf{e}}_{i-1}$ and $\hat{\mathbf{e}}_i$ respectively. Then, $\hat{\mathbf{t}}_{i+1} = \hat{\mathbf{e}}_i \times (\hat{\mathbf{e}}_{i-1} \times \hat{\mathbf{e}}_i)$, $\hat{\mathbf{t}}_{i-1} = \hat{\mathbf{e}}_{i-1} \times (\hat{\mathbf{e}}_{i-1} \times \hat{\mathbf{e}}_i)$. If $\hat{\mathbf{e}}_{i-1} \cdot \hat{\mathbf{e}}_i \geqq 0$, $\alpha = \arcsin(||\hat{\mathbf{e}}_{i-1} \times \hat{\mathbf{e}}_i||)$. If $\hat{\mathbf{e}}_{i-1} \cdot \hat{\mathbf{e}}_i < 0$, $\alpha = \pi - \arcsin(||\hat{\mathbf{e}}_{i-1} \times \hat{\mathbf{e}}_i||)$. The torsional spring force can be computed as follows:

$$\mathbf{f}_{i-1} = k_{ts}\frac{\alpha}{\pi||P_{i-1} - P_i||}\hat{\mathbf{t}}_{i-1}, \quad (7)$$

$$\mathbf{f}_{i+1} = k_{ts}\frac{\alpha}{\pi||P_{i+1} - P_i||}\hat{\mathbf{t}}_{i+1}, \quad (8)$$

$$\mathbf{f}_i = -(\mathbf{f}_{i-1} + \mathbf{f}_{i+1}). \quad (9)$$

where k_{ts} is the torsional spring constant.

4) Torsional damper: The torsional damper works against the torsional spring to prevent any harmonic motion from accumulating. Similar to the linear damper, it also models the internal friction that resists bending in regular objects. Let, v_{i-1}, v_{ib}, be the norms of the velocity components of, $\mathbf{v}_{i-1}$, and, $\mathbf{v}_i$, on the direction of, $\hat{\mathbf{t}}_{i-1}$, and let, v_{i+1}, v_{ia}, be the norms of the velocity components of, $\mathbf{v}_{i+1}$, and, $\mathbf{v}_i$, on the direction of, $\hat{\mathbf{t}}_{i+1}$, Then, the torsional damper on the points, P_{i-1}, P_i and P_{i+1}, can be computed by:

$$\mathbf{f}_{i-1} = (\frac{(v_{i-1} - v_{ib})}{||P_{i-1} - P_i||} + \frac{(v_{i+1} - v_{ia})}{||P_{i+1} - P_i||})\frac{k_{td}\hat{\mathbf{t}}_{i-1}}{||P_{i-1} - P_i||}, \quad (10)$$

$$\mathbf{f}_{i+1} = (\frac{(v_{i-1} - v_{ib})}{||P_{i-1} - P_i||} + \frac{(v_{i+1} - v_{ia})}{||P_{i+1} - P_i||})\frac{k_{td}\hat{\mathbf{t}}_{i+1}}{||P_{i+1} - P_i||}, \quad (11)$$

$$\mathbf{f}_i = -(\mathbf{f}_{i-1} + \mathbf{f}_{i+1}). \quad (12)$$

where k_{td} is torsional damper constant, $v_{i-1} = \mathbf{v}_{i-1} \cdot \hat{\mathbf{t}}_{i-1}$, $v_{ib} = \mathbf{v}_i \cdot \hat{\mathbf{t}}_{i-1}$, $v_{i+1} = \mathbf{v}_{i+1} \cdot \hat{\mathbf{t}}_{i+1}$, $v_{ia} = \mathbf{v}_i \cdot \hat{\mathbf{t}}_{i+1}$.

5) Swivel damper: Point, P_{i-1}, has a velocity relative to the center point, P_i. So far, two components of that relative velocity have been dampened. There still remains a component perpendicular to those two. Without the dampening, point P_{i-1} could indefinitely orbit the line formed by extending the edge connecting point P_{i+1} and point P_i (See (b) of Fig. 3).

Let $\hat{\mathbf{s}}$ be the unit vector of the swivel dampers of point P_{i-1} and P_{i+1}, then, $\hat{\mathbf{s}} = \hat{\mathbf{e}}_{i-1} \times \hat{\mathbf{e}}_i$. The swivel dampers can be computed by:

$$\mathbf{f}_{i-1} = k_{sw}\frac{(\mathbf{v}_{i-1} - \mathbf{v}_i) \cdot \hat{\mathbf{s}}}{||P_{i-1} - P_i||}\hat{\mathbf{s}}, \quad (13)$$

$$\mathbf{f}_{i+1} = k_{sw}\frac{(\mathbf{v}_{i+1} - \mathbf{v}_i) \cdot \hat{\mathbf{s}}}{||P_{i+1} - P_i||}\hat{\mathbf{s}}, \quad (14)$$

$$\mathbf{f}_i = -(\mathbf{f}_{i-1} + \mathbf{f}_{i+1}). \quad (15)$$

where k_{sw} is the swivel damper constant.

IV. Force Propagation Along the Suture

To prevent our suture from being stretched too long or compressed too short, we set l_{max} and l_{min} as the maximum and minimum length of one suture segment respectively.Let l_i be the segment length between P_i and P_{i+1}. To analyze the force propagation when the user grabs the suture, we need to compute the forces acting at each point from the grabbed point to the start point and to the end point of the suture. We define different scenarios as follows:

A. Condition A

Assume the user grabs point P_{i+1} with one hand. If $l_{min} < l_i < l_{max}$. There is no propagation of the user input force $\mathbf{f}_h$ from point P_{i+1} to P_i. All the user input force has been converted to the internal forces along the suture.

B. Condition B

Assume the user grabs point P_{i+1} with one hand. If the expected segment length $l_i' > l_{max}$ or $l_i' < l_{min}$, we need to adjust the segment length to l_{max} or l_{min} (see (a) of Fig. 4).

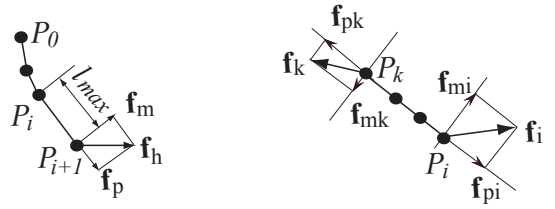

(a) *One-Hand Pulling* (b) *Two-Hand Pulling*

Fig. 4. Force Propagation

Let $\mathbf{f}_p$ be the component of the input force $\mathbf{f}_h$ along the segment direction, and $\mathbf{f}_p$ is the input force propagated to point P_i from point P_{i+1}. $\mathbf{f}_p$ and $\mathbf{f}_m$ can be obtain from the following equations:

$$\mathbf{f}_p = (\mathbf{f}_h \cdot \hat{\mathbf{e}}_i)\hat{\mathbf{e}}_i, \quad (16)$$

$$\mathbf{f}_m = (\mathbf{f}_h \cdot \hat{\mathbf{e}}_m)\hat{\mathbf{e}}_m. \quad (17)$$

where $\hat{\mathbf{e}}_m = \frac{\hat{\mathbf{e}}_i \times \mathbf{f}_h}{||\hat{\mathbf{e}}_i \times \mathbf{f}_h||} \times \hat{\mathbf{e}}_i$, $\hat{\mathbf{e}}_i$ can be obtain from equation (5). Using the same method as above, we can derive the user input force propagated at each point of the suture.

C. Condition C

In this condition, we assume the user is pulling two points,P_k and P_i, of the suture. The method is almost the same as in condition B. But we need to do the propagation computation twice, first starting from point P_i, and then starting from point P_k (see (b) of Fig. 4).

V. Case Study and Result

A. Collision Detection and Management

First, we build a bounding-volume hierarchy (BVH) from the bottom-up representing the shape of the rope at successive levels of detail. This method is similar to the method proposed in [16]. To find the self-collisions of the rope, we explore two copies of the BVH from the top down. Whenever two BVHs (one from each copy) are found to not overlap, we know that they cannot contain colliding segments, and hence, we do not explore their contents. When two leaf spheres overlap, the distance between the two centers of the nodes is computed. If it is less than the node diameter, $2r$, then the two segments are reported to collide. However, no node is ever considered to be in collision with itself or its immediate neighbors along the suture chain.

To find the collisions between the rope and grippers, we consider the gripper as line segments with a given radius, and check if the BHV of the rope has any overlap with the line segments.

When two suture segments are detected to be at a distance $d < 2r$ from each other, then, an equal (but opposite) displacement vector is applied to each segment along. This displacement is just long enough to take the segments out of collision, with a slight "safety margin". Hence, each node is shifted away by $r - d/2 + \varepsilon/2$.

If a collision occurred, during real time simulation, we need to compute new velocities of mass points which are involved in the collision. Similarly to the method presented in [17], we apply impulses to the end points of these two segments. See Fig. 2 for the case where point C with relative position a along the segment $\overrightarrow{P_aP_b}$ interacts with point E with relative position b along the segment $\overrightarrow{P_cP_d}$. Let $\mathbf{i}$ be the impulse, then, $\mathbf{i} = \mathbf{n}\Delta t$. where $\mathbf{n}$ is the repulsion force that we can obtain from equation (3). Then we can compute the new velocities as follows:

$$i' = \frac{2||\mathbf{i}||}{(a^2+b^2+(1-a)^2+(1-b)^2)}, \quad (18)$$

$$\mathbf{v}_a^{new} = \mathbf{v}_a + (1-a)\frac{i'}{m}\hat{\mathbf{n}}, \quad (19)$$

$$\mathbf{v}_b^{new} = \mathbf{v}_b + a\frac{i'}{m}\hat{\mathbf{n}}, \quad (20)$$

$$\mathbf{v}_c^{new} = \mathbf{v}_c - (1-b)\frac{i'}{m}\hat{\mathbf{n}}, \quad (21)$$

$$\mathbf{v}_d^{new} = \mathbf{v}_d - b\frac{i'}{m}\hat{\mathbf{n}}. \quad (22)$$

where m is the mass of each mass point P_a, P_b, P_c, and P_d. $\hat{\mathbf{n}}$ is the unit vector from point E to point C.

B. Experiment Setup

Our simulation was implemented on a PC with dual 3.2G Intel®Pentium®4 CPUs and 512 MB memory. For physics-based models, the most challenging part is how to determine its parameters. If parameters are inappropriate, it may impact the whole system's stability or even over its limits. After many experiments, we chose our suture parameters as in Table I:

TABLE I
Suture Parameter Setting

Parameter	Value	Remarks
N	$20 \sim 50$	Number of Points
l	$5.0m$	Length of the suture
r	$0.05m$	Radius of the suture
m	$0.05kg$	mass of one point
G	$9.8N/kg$	Gravity
k_h	1200	Virtual coupling spring constant
s	0.003	Scale factor for output force
μ	10	Friction constant
k_{rs}	100	Repulse spring constant
k_{rd}	5	Repulse spring damper constant
k_l	800	Linear spring constant
k_d	1	Linear damper constant
k_{ts}	10	Torsional spring constant
k_{td}	0.05	Torsional damper constant
k_{sw}	0.2	Swivel damper constant

With the parameters above, we can obtain around $500Hz \sim 1000Hz$ update rate for both Phantom Omnis. Users can feel the output forces of smooth quality.

C. Experiment of Knotting

We build five different models with various combinations of forces models described in section III. With two PHANTOM Omni haptic devices, users can tie an arbitrary knot about the suture which is hung up on one fixed frame (see Fig. 5).

Fig. 5. A user is tying knot with two PHANTOM Omnis

1) Model 1: This model contains only a linear spring and a linear damper. It is the least realistic model. The two connected segments can bend to any angle effortlessly.

TABLE II
SCREEN SHOTS OF DIFFERENT MODELS

Model	Screen Shot 1	Screen Shot 2
1	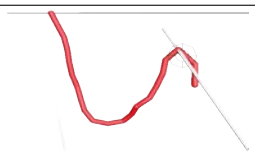	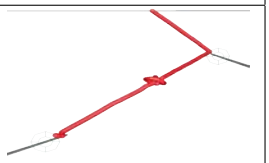
2	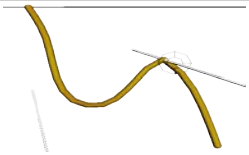	
3	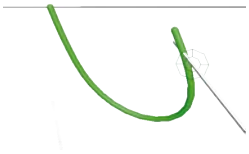	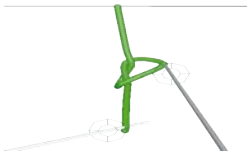
4		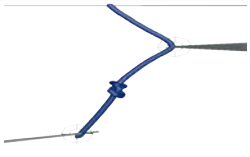
5	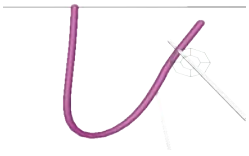	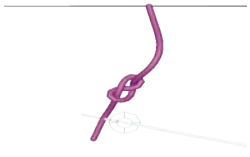

2) Model 2: This model is almost the same as model 1, but also contains a torsional spring. The torsional spring adds a lot more realistic behaviour to the thread, but also, because it uses a nonlinear function 'acos', it creates some harmonic wave motions.

3) Model 3: Compared to model 2, a torsional damper has been added to this model. This damper stops the harmonic motion presented in model 2. But this model creates another class of instability where it is very sensitive to the thread and creates a self-excitation phenomenon.

4) Model 4: This model includes a 'swivel' damper to fix the problem of perpetual orbiting (the self excitation mentioned in the above). The result is a thread that looks more like a real thread.

5) Model 5: This model has all the components of model 4. The only difference is that the linear spring's force computed quadratically on the difference between its current length and rest length, instead on linearly. This makes the thread appear a lot less stretchy, which is more realistic since the real threads stretch very little. The thread's non-linear response also makes it a lot more responsive to movements.

Comparing the results from above five different models (See TABLE II for the comparison), we can draw a conclusion that model 4 is the most ideal model for our surgical training environment.

D. Experiment of Force Propagation

Because the maximum exertable face for PHANTOM Omni is 0.75lbf (3.3N), we can not output the forces to the Haptic devices from virtual coupling spring directly. Therefore, we chose a constant equal to 0.003 to scale the forces before we feed them to PHANTOM Omnis. We plot the forces which we send to PHANTOM Omni during each haptic update frame for both one-hand pulling and two-hand pulling cases. Taking the magnitudes of the forces as y-axis and each haptic update frame as x-axis, we obtain the forces plots as in TABLE III.

E. Experiment of Unknotting

Same as the knotting experiment, the suture is hung up on one fixed frame. Also, to make knotting and unknotting easier, we set up a desk under the suture model to let part of the suture lay on the desk.In order to untie a knot successfully, we have to pick up the right point, otherwise the knot could be more tightening instead of loosening. This is part of the unknotting planning algorithm which will not be discussed here. Fig. 6 show the successful unknotting of a figure-of-eight knot. Fig. 7 shows if you grab the wrong point, the knot can not be untied.

VI. CONCLUSION AND FUTURE WORK

We presented a fast and simple approach to compute 3D DLO simulations. We simulate both internal forces and external forces. Also, we analyzed how forces propagate along the suture when the user pulls the suture with one hand or two hands. While our simulation cannot produce physically exact shapes and forces, even sometimes the user

TABLE III
FORCE PLOTS OF SUTURING PULLING

Screen Shot	Force Plot
	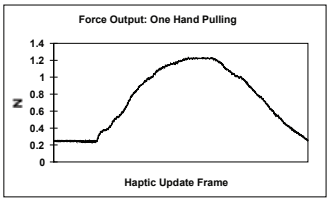
	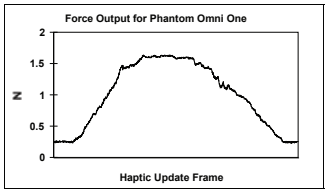
	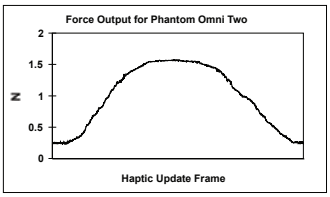

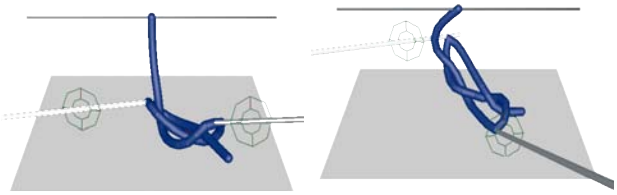

Fig. 6. Unknot a figure-of-eight knot

might feel the force feedback a little unstable (because of the high demanding of the haptic device refresh rate), our methods can be used in virtual reality simulation to give users more realistic senses.

Because our model is based on the finite element method, to make sutures more realistic, we must add more segments and more mass points to the model, which may cause the program run more slowly (the more mass points the model has, the more time we need to complete dynamic computation and collision detection). Therefore, we cannot guarantee the haptic rendering rate to be around 1000Hz. Users may feel the force output less smooth sometimes. To solve the problem mentioned above, we may introduce level of detail methods to the modeling and undertake some optimization of dynamic computation and collision detection methods. Also, to speed-up the operation, we will look into Physics Process Unit (PPU) for the case of suturing and knotting in surgical training environment. In this paper, we did not consider the static friction, our next step is to study the forces when the user is trying to tie a knot tightly and untie a tight knot.

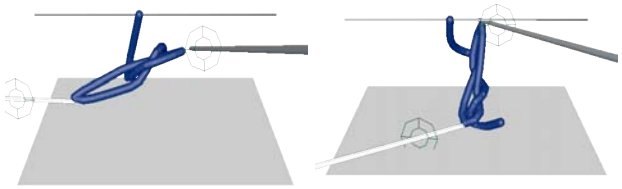

Fig. 7. Unsuccessful unknotting

REFERENCES

[1] H. Wakamatsu, E. Arai, S. Hirai, *Knotting/Unknotting Manipulation of Deformable Linear Objects*, International Journal of Robotics Research, Volume 25 , Issue 4 (April 2006), Pages: 371 - 395, ISSN:0278-3649

[2] H. Wakamatsu, K. Takahashi, S. Hirai, *Dynamic Modeling of Linear Object Deformation based on Differential Geometry Coordinates* Robotics and Automation, 2005. ICRA 2005. Proceedings of the 2005 IEEE International Conference on Publication Date: 18-22 April 2005 On page(s): 1028- 1033 ISBN: 0-7803-8914-X

[3] J. Takamatsu, T. Morita, K. Ogawara, H. Kimura, K. Ikeuchi, *Representation for Knot-Tying Tasks*, Robotics, IEEE Transactions,Volume: 22, Issue: 1,On page(s): 65- 78,Feb. 2006

[4] M. Saha, P. Isto, *Motion planning for robotic manipulation of deformable linear objects* Robotics and Automation, 2006. ICRA 2006. Proceedings 2006 IEEE International Conference on May 15-19, 2006 Page(s):2478 - 2484

[5] D. Pai, *Strands: Interactive simulation of thin solids using cosserat models*, Computer Graphics Forum, 21(3):347–352, 2002. Proceedings of Eurographics'02.

[6] C. Wang, A.M.D. Richardson, D. Liu, R. Rosing, R. Tucker and B. De Masi, *Construction of Nonlinear Dynamic MEMS Component Models Using Cosserat Theory*, Proc. SPIE Design, Test, Integration & Packaging of MEMS Symposium, 2003

[7] D. Q. Cao, Dongsheng Liu, Charles H.-T. Wang, *Three Dimensional Nonlinear Dynamics of Slender Structures: Cosserat Rod Element Approach*, eprint arXiv:math/0410286,10/2004

[8] M. Grgoire, E. Schmer, *Interactive simulation of one-dimensional flexible parts*, Proceedings of the 2006 ACM symposium on Solid and physical modeling. Pages: 95 - 103 Year of Publication: 2006 ISBN:1-59593-358-1

[9] J. Phillips, A. Ladd and L.E. Kavraki, *Simulated knot tying*, Robotics and Automation, 2002. Proceedings. ICRA '02. IEEE International Conference on Volume 1, 11-15 May 2002 Page(s):841 - 846 vol.1

[10] B. Kahl, D. Henrich, *Manipulation of deformable linear objects: Force-based simulation approach for haptic feedback*, 12th International Conference on Advanced Robotics (ICAR 2005), July 18th-20th, 2005

[11] F. Wang, E. Burdet, A. Dhanik, T. Poston, , C. L. Teo , *Dynamic Thread for Real-Time Knot-Tying*, Proceedings of the First Joint Eurohaptics Conference and Symposium on Haptic Interfaces for Virtual Environment and Teleoperator Systems - Volume 00 2005

[12] M. LeDuc, S. Payandeh, J. Dill, *Toward modeling of a suturing task*, Graphics Interface (GI), pp 273-279, Halifax, Nova Scotia, 2003.

[13] J.E. Colgate, M.C. Stanley, J.M. Brown, *Issues in the haptic display of tool use*, Intelligent Robots and Systems 95. 'Human Robot Interaction and Cooperative Robots', Proceedings. 1995 IEEE/RSJ International Conference on Publication Date: 5-9 Aug 1995

[14] J. Lenoir, P. Meseure, L. Grisoni, C. Chaillou, *A suture model for surgical simulation*, 2nd International Symposium on Medical Simulation (ISMS'04) pp. 105-113, Cambridge, Massachusetts (USA).

[15] J. Lenoir, P. Meseure, L. Grisoni, C. Chaillou, *Surgical thread simulation*, Modelling & Simulation for Computer-aided Medicine and Surgery, (MS4CMS), November 2002

[16] J. Brown, J. Latombe, K. Montgomery, *Real-time knot tying simulation*, The Visual Computer: International Journal of Computer Graphics, 20(2): 165-179.

[17] R. Bridson, R. Fedkiw, J. Anderson, *Robust treatment of collisions, contact and friction for cloth animation*, Proceedings of the 29th annual conference on Computer graphics and interactive techniques. Pages: 594 - 603 Year of Publication: 2002 ISBN ISSN:0730-0301, 1-58113-521-1